

Global Stock Market Volatility Forecasting Incorporating Dynamic Graphs and All Trading Days

Zhengyang CHI*, Junbin GAO, and Chao WANG†

Discipline of Business Analytics, The University of Sydney Business School,

The University of Sydney, Camperdown, NSW 2006, Australia

October 2, 2024

arXiv:2409.15320v2 [q-fin.GN] 1 Oct 2024

*Corresponding author. Email: zhengyang.chi@sydney.edu.au

†Email for all authors: {zhengyang.chi, junbin.gao, chao.wang}@sydney.edu.au

Abstract

This study introduces a global stock market volatility forecasting model that enhances forecasting accuracy and practical utility in real-world financial decision-making by integrating dynamic graph structures and encompassing the union of active trading days of different stock markets. The model employs a spatial-temporal graph neural network (GNN) architecture to capture the volatility spillover effect, where shocks in one market spread to others through the interconnective global economy. By calculating the volatility spillover index to depict the volatility network as graphs, the model effectively mirrors the volatility dynamics for the chosen stock market indices. In the empirical analysis, the proposed model surpasses the benchmark model in all forecasting scenarios and is shown to be sensitive to the underlying volatility interrelationships.

Keywords: Realized Volatility Forecasting; Multivariate Time Series Forecasting; Spatiotemporal Analysis; Dynamic Graph Neural Networks

1 Introduction

Volatility is critical in financial applications, particularly for managing investment risks and derivative pricing. In contrast to the backward-looking perspective of using historical volatility, performing volatility forecast is more insightful and relevant because it provides forward-looking estimates that reflect current market conditions and potential future events. Hence, accurate volatility forecasting is a meaningful research topic.

Salient attributes, such as the clustering phenomenon and the mean reversion behavior, of the financial volatility are well documented by the literature ([Poon and Granger, 2003](#)). Among these attributes, the comovement and correlation among the volatility in different stock markets globally have received increasing attention from both researchers and practitioners. Especially, the volatility spillover effect has been frequently discussed in the literature (e.g., ([Kanas, 2000](#)), ([Forbes and Rigobon, 2002](#)), ([Diebold and Yilmaz, 2009](#)), ([Yang and Zhou, 2017](#)), ([Bollerslev et al., 2018](#))). It provides the theoretical foundations

on how volatility changes in one market can precipitate similar changes in others. For instance, the volatility spillover effects can measure how the increase or decrease of the volatility of certain stock markets can cause the increase or decrease of the volatility of other stock markets globally. Such interdependencies highlight the complexity of global financial systems and the need for sophisticated analytical models.

Graph Neural Networks (GNNs) are a type of neural network designed to learn from data structured as graphs. They can proficiently capture the relationships and interactions between different nodes (entities) within these graphs through neural network layers that iteratively aggregate and transform information from neighboring nodes. This process allows GNNs to learn complex patterns in the graph structure and makes them suitable for tasks where relationships are important. When analyzing interdependent time series, GNNs are particularly effective. The series can be modeled as nodes in a graph with their relationships represented as edges. This enables the model to learn from both individual time series and their mutual influences, thus generating more accurate forecasts based on interconnected dynamics. This research aims to design a tailored multivariate dynamic GNN framework to effectively capture the spillover effect across global markets, via modeling the volatility data in both sequential and relational domains. The proposed model should improve the accuracy and utility of multivariate volatility forecasting and provide insights into the interconnection of different global financial markets.

This paper is structured as follows. Section 2 reviews of the relevant literature. Section 3 outlines the motivation behind this research. Section 4 elaborates on the methods and practical implementation of the proposed model. Detailed information about the experiments is presented in Section 5, and the relevant codes are accessible at <https://github.com/MikeZChi/DCRNN-RV.git>. Finally, Section 6 concludes the paper.

2 Literature Review

The purpose of this review section is to establish a clear understanding of volatility measurement and explore various univariate and multivariate models for forecasting financial volatility.

2.1 Volatility Measurement

Volatility cannot be directly observable because it involves the inherent variability of a security or market's returns over a time period. However, different types of volatility measurements have been proposed to estimate the volatility ([Wilmott, 2013](#)). Although they should be identical in essence that all of them represent or estimate the same variable, their values may differ from each other in practice ([Mitra, 2009](#)). Here, the target volatility measurement, the Realized Volatility (RV) used in the proposed model, is reviewed in this section.

RV is proposed by [Andersen and Bollerslev \(1998\)](#). The volatility at time t can be theoretically detected through the sample track of the return with sufficiently high sampling frequency. Given the availability of such high-frequency data, RV can be used to depict the daily volatility on day t because it is derived from the aggregated high-frequency intraday returns.

$$RV_t = \sum_{m=1}^M r_{m,t}^2, \quad (1)$$

where RV_t is the RV on day t , $r_{m,t}$ represents the m -th intraday high-frequency return on day t , and the sampling frequency is $\frac{1}{M}$.

The proposed model of this research aims at the RV forecast problem because the RV of a stock market index on day t can be regarded as the daily volatility of the market on day t .

2.2 Univariate and Multivariate Volatility Forecasting

Given that the proposed model performs RV forecast, discussions on volatility forecasting methods are limited to relevant RV-focused models only. The Heterogeneous Autoregressive (HAR) model, proposed by [Corsi \(2009\)](#) and improved by [Bollerslev et al. \(2018\)](#), is one of the most commonly used models in RV forecasting. Here, since the discussions focus on RV forecasting, the HAR model will be denoted as HAR-RV. The HAR-RV model also has multiple extensions, which are covered in this section.

The HAR-RV model identifies the overall pattern of volatility across three distinct time intervals. It uses the pooled panel data consisting of the past daily, past weekly and past monthly RV to forecast the future RV. These three inputs are expected to reflect the short-term, mid-term and long-term behaviors of the investors, respectively. Assuming that the high-frequency daily RV data are available, the forecast task is to predict $RV_{i,t}$ for each of the N selected stock markets. Hence, the univariate HAR-RV model for individual stock market i ($i = 1, 2, \dots, N$) can be formulated as:

$$RV_{i,t} = \alpha_i + \beta_{i,d}RV_{i,t-1} + \beta_{i,w}RV_{i,t-5:t-1} + \beta_{i,m}RV_{i,t-22:t-1} + \epsilon_{i,t}, \epsilon_{i,t} \sim N(0, \sigma_{\epsilon_i}^2), \quad (2)$$

where $RV_{i,t-n:t-1} = \frac{1}{n} \sum_{j=t-n}^{t-1} RV_{i,j}$ is the mean RV of the i^{th} stock market from time $t-1$ to time $t-n$. Here, the $\beta_{i,d}$, $\beta_{i,w}$ and $\beta_{i,m}$ are scalars which, for each stock market, represent the past daily, weekly and monthly impact on forecasting future RVs. Besides, the α_i is also a scalar. The log-transformed version and the square root of the RV data are commonly used in the HAR-RV model to deliver better forecasting performances because the original RV data typically exhibits skewness and leptokurtosis (fat tails).

Although the forecast capability is improved with the transformed version of RV, the univariate HAR-RV model fails to capture the relationships between the volatility of different stock markets. It forecasts the RV of each observed stock market in an isolated manner, which is regarded as biased given the salient phenomenon of the volatility spillover effect.

To account for multivariate RV forecasting, $\mathbf{v}_t = [\text{RV}_{1,t}, \text{RV}_{2,t}, \dots, \text{RV}_{N,t}] \in \mathbb{R}^N$ is used to denote the RV observations for all the entities at time t . Proposed by [Bubák et al. \(2011\)](#), the Vector HAR-RV (VHAR-RV) model captures the relationship among the RV panel data of several European foreign exchange markets as a multivariate HAR-RV model. The model can be formulated in the following:

$$\tilde{\mathbf{v}}_t = \boldsymbol{\alpha} + \boldsymbol{\beta}_d \tilde{\mathbf{v}}_{t-1} + \boldsymbol{\beta}_w \tilde{\mathbf{v}}_{t-5:t-1} + \boldsymbol{\beta}_m \tilde{\mathbf{v}}_{t-22:t-1} + \boldsymbol{\epsilon}_t, \boldsymbol{\epsilon}_t \sim N(0, \boldsymbol{\Sigma}_\epsilon^2), \quad (3)$$

where $\tilde{\mathbf{v}}_t = [\text{RV}_{1,t}^{\frac{1}{2}}, \text{RV}_{2,t}^{\frac{1}{2}}, \dots, \text{RV}_{N,t}^{\frac{1}{2}}]$ represents the square root of RV and $\boldsymbol{\beta}_d$, $\boldsymbol{\beta}_w$ and $\boldsymbol{\beta}_m$ are $\mathbb{R}^{N \times N}$ matrices to capture the interplay between different markets. These square matrices of trainable parameters allow the model to learn the joint behavior of the RV data in different stock markets. However, the model can only learn linear relationships. Besides, as the number of parameters increases from 3 to $3N^2$, the linear HAR model becomes much more complicated which may lead to problems such as overfitting.

The HAR-RV-KS model is proposed by [Liang et al. \(2020\)](#) to incorporate the relational information between stock markets into the univariate HAR-RV model. The ‘KS’ represents Kitchen Sink and means that the model includes a variety number of features. Specifically, the HAR-RV-KS adds the past daily RV data of other stock market indices to the HAR-RV model. The HAR-RV-KS employs the square root of the RV as well. The forecast model for each individual stock market i can be formulated below:

$$\begin{aligned} (\text{RV}_{i,t})^{1/2} = & \beta_{i,0} + \beta_{i,d} (\text{RV}_{i,t-1})^{1/2} + \beta_{i,w} (\text{RV}_{i,t-5:t-1})^{1/2} \\ & + \beta_{i,m} (\text{RV}_{i,t-22:t-1})^{1/2} + \sum_{k \in \{1, \dots, N\} \setminus \{i\}} \beta_{k,d} (\text{RV}_{k,t-1})^{1/2} + \varepsilon_{i,t}, \end{aligned} \quad (4)$$

where k is the index of different entities involved in the volatility system and their lagged daily RV values are treated as additional attributes for the HAR-RV-KS model. Through adding extra features and coefficients, the relationship between the different stock markets can be learned through training. However, the HAR-RV-KS also suffers from the

overfitting problem, even though this problem can be partially alleviated by replacing the extra feature aggregation with the first principle component of the past daily RV data (Liang et al., 2020). Furthermore, this model assumes the volatility interdependence between stock markets is linear and is limited to one time period lag. This assumption is inappropriate because the persistence and the long-term memory characteristics of the volatility behavior are well recognized (Poon and Granger, 2003).

Instead of learning the relationship network through training, the Graph HAR (GHAR) is proposed by Zhang et al. (2023) to capture the volatility spillover effect based on the graph structure captured by the Graphical LASSO (GLASSO) method (Friedman et al., 2007) before the actual training procedure to enhance the efficiency of the model. The precision matrix derived through the GLASSO algorithm is transformed and used as the adjacency matrix for the volatility relationship graph. Following the ‘KS’ manner, the GHAR model directly adds its graph design to the HAR-RV model with slight modifications on the time interval of the mid-term and long-term RV data to avoid overlapping:

$$\begin{aligned} \mathbf{v}_t &= \boldsymbol{\alpha} + \beta_d \mathbf{v}_{t-1} + \beta_w \mathbf{v}_{t-5:t-2} + \beta_m \mathbf{v}_{t-22:t-6} \\ &+ \gamma_d \mathbf{D}^{-\frac{1}{2}} \mathbf{A} \mathbf{D}^{-\frac{1}{2}} \mathbf{v}_{t-1} + \gamma_w \mathbf{D}^{-\frac{1}{2}} \mathbf{A} \mathbf{D}^{-\frac{1}{2}} \mathbf{v}_{t-5:t-2} + \gamma_m \mathbf{D}^{-\frac{1}{2}} \mathbf{A} \mathbf{D}^{-\frac{1}{2}} \mathbf{v}_{t-22:t-6} \\ &+ \boldsymbol{\epsilon}_t, \end{aligned} \quad (5)$$

where $\mathbf{A} \in \mathbb{R}^{N \times N}$ is the estimated adjacency matrix constructed based on the precision matrix from the GLASSO algorithm and $\mathbf{D} \in \mathbb{R}^{N \times N}$ is the diagonal matrix $\mathbf{D} = \text{diag}(d_1, \dots, d_N)$, in which $d_i = \sum_{j=1}^N A_{ij}$. Besides, β_d , β_w and β_m are the impact of the lagged panel RV observations similar to the HAR-RV model, whereas the γ_d , γ_w and γ_m measure the influence from the past RV values from the neighborhood entities. In the GHAR model, the volatility spillover effect is still depicted as linear. In addition, it only considers the effect of the direct neighborhood. To improve the GHAR model, Zhang et al. (2023) further proposed the GNNHAR model to capture the nonlinear volatility spillover effect in the broader neighborhood by replacing the graph design in the GHAR with a multilayer Graph Convolutional Network (GCN). A l -layer GNNHAR

can be formulated as:

$$\begin{aligned}
\mathbf{H}^{(0)} &= [\mathbf{v}_{t-1}, \mathbf{v}_{t-5:t-2}, \mathbf{v}_{t-22:t-6}], \\
\mathbf{H}^{(1)} &= \text{ReLU}(\mathbf{D}^{-\frac{1}{2}} \mathbf{A} \mathbf{D}^{-\frac{1}{2}} \mathbf{H}^{(0)} \Theta^{(l)}), \\
&\dots, \\
\mathbf{H}^{(l+1)} &= \text{ReLU}(\mathbf{D}^{-\frac{1}{2}} \mathbf{A} \mathbf{D}^{-\frac{1}{2}} \mathbf{H}^{(l)} \Theta^{(l)}), \\
\mathbf{v}_t &= \boldsymbol{\alpha} + \beta_d \mathbf{v}_{t-1} + \beta_w \mathbf{v}_{t-5:t-2} + \beta_m \mathbf{v}_{t-22:t-6} \\
&\quad + \boldsymbol{\gamma} \mathbf{H}^{(l+1)} + \boldsymbol{\epsilon}_t,
\end{aligned} \tag{6}$$

where $\boldsymbol{\gamma} = [\gamma_d, \gamma_w, \gamma_m]$. In contrast to equation (5), equation (6) includes nonlinearity and considers a broader neighborhood in modeling the interconnected volatility dynamics.

In volatility forecast, the power of the GNN models is further explored by [Son et al. \(2023\)](#) through leveraging a spatial-temporal GNN model, Diffusion Convolutional Recurrent Neural Network (DCRNN), proposed by [Li et al. \(2018\)](#). This model is originally designed to address the challenges in traffic forecasting by integrating spatial and temporal dependencies. The DCRNN model uses diffusion convolution to model spatial dependencies as a diffusion process on a directed graph and employs Gated Recurrent Units (GRU) as a variant of typical recurrent neural networks (RNNs) to capture temporal dynamics of traffic flow. The model also applies the encoder-decoder architecture for improved long-term forecasting. This model is applied to RV forecast on eight different stock markets and achieves satisfactory results compared to the HAR-RV family models in all the short-term, mid-term and long-term forecasting tasks ([Son et al., 2023](#)). In the RV forecast application, the model is denoted as the STG-Spillover model. Similar to the GNNHAR model, the volatility relational graph is constructed before the STG-Spillover model is trained. The volatility spillover effect is captured through the Diebold & Yilmaz (DY) framework proposed by [Diebold and Yilmaz \(2012\)](#). Compared to the GLASSO method or other methods such as using the Pearson correlation coefficients, the DY framework is more suitable for the RV data and can better capture the asymmetry in

the volatility spillover effect. The details of the DY framework and the DCRNN model are discussed in later sections.

3 Research Motivation

From the HAR-RV to the DCRNN model, great efforts have been made to utilize the interdependence between markets or assets to increase forecasting accuracy. Experiments have also been conducted to empirically prove the superiority of multivariate RV forecast over univariate RV forecast (Zhang et al., 2023; Son et al., 2023). However, the limitations of all the current state-of-the-art multivariate RV forecast models are discussed below.

The first limitation is that all the multivariate RV forecast models are performed on common trading days. This can significantly limit the sample size of the multivariate RV forecast when cross-market investments are interesting to investors. For example, a RV dataset of multiple stock markets¹ contains the RV data of 31 stock market indices from January 2000 to June 2022. For stock market indices such as FCHI and SPX, both of them have more than 5500 observations within the selected period. On the contrary, some stock market indices, like OMXSPI, have only 4195 observations. The number of common trading days for eight market indices, SPX, GDAXI, FCHI, FTSE, OMXSPI, N225, KS11 and HSI, from October 2006 to June 2022 is 3311. In contrast, the union of the trading days of these eight stock markets includes more than 4000 dates for the same period. This difference is expected to increase when more stock market indices or larger time windows are taken into consideration. Multivariate RV forecast models are generally less data-efficient compared to univariate ones, which leads to higher costs associated with their use in practice. In addition, the h -step ahead forecast results of the current multivariate RV forecast models is the forecast RV of the next h common trading days, instead of the next h trading days, of the selected markets. This limitation further impairs the effectiveness of multivariate RV forecast models in practice. Investors and

¹This dataset can be obtained on request.

portfolio managers need accurate RV forecasts not only for common trading days but also for uncommon ones, especially when their investments are concentrated in a specific market but need insights from a broader range of markets to make informed decisions.

The second limitation is that current multivariate RV forecast models only stick to fixed volatility spillover relational graphs. This means that no matter how long a period is selected, the interdependence pattern between different stock markets is always fixed. This could be further improved, especially for the volatility dynamics. Many time-varying factors could be influential to the potential volatility dynamics, including policy evolution, the common global crisis, the different local disasters, the divergent development trajectories of different markets and so forth.

By proposing a more dynamic and flexible GNN-based model, this research aims to address the limitations mentioned above and to enhance the utility and power of multivariate RV forecasts. Hence, this research is motivated by these limitations and aims to propose a more dynamic and flexible model. Given the flexibility and expressiveness requirement for the desired model, this research also employs DCRNN as it is a powerful model that can learn from both relational and sequential data. Compared to the traditional HAR-RV family of models, the DCRNN model allows more complex transformations to incorporate desired designs. The research aims to further explore the potential of the DCRNN model, especially in its capability to effectively learn from multiple RV time series. In addition, through fully leveraging the information contained in the RV data by including uncommon trading days and the changing volatility network structure, this research also aims to reveal new dimensions of the volatility interconnectivity between markets and enhance the understanding of stock market volatility dynamics.

4 Methodology and Implementation

This section introduces the detailed design of the proposed model. Particularly, the general graph learning methodology, the strategy to incorporate uncommon trading days into the dataset and the method to learn from a time-varying adjacency matrix are discussed in detail. In general, the proposed model can be seen as an extension of the DCRNN model with necessary revisions and transformations applied for better multivariate RV forecasts. The proposed model is called the DCRNN-RV model.

4.1 Graph Learning for Relational Data

Suppose the graph $\mathcal{G} = (\mathcal{V}, \mathcal{E})$ consists of N nodes, where \mathcal{V} and \mathcal{E} denote the set of nodes and the set of edges in the graph, respectively. Furthermore, $v_i \in \mathcal{V}$ represents the i^{th} node within the node set and $e_m = (v_i, v_j) \in \mathcal{E}$ denotes the m^{th} edge between node v_i and node v_j within the edge set. Here, matrix $\mathbf{X} \in \mathbb{R}^{N \times D}$ can be used to denote the collection of the features of all nodes. Especially, each row of matrix \mathbf{X} is the node feature vector $\mathbf{x}_i \in \mathbb{R}^D$ of node v_i . In addition, the adjacency matrix \mathbf{A} and degree matrix \mathbf{D} can be used to measure the relationships or interactions between nodes and store the structural information of the corresponding graph. For example, consider \mathcal{G} as a simple undirected and unweighted graph. Both the adjacency matrix $\mathbf{A} \in \mathbb{R}^{N \times N}$ and the degree matrix $\mathbf{D} \in \mathbb{R}^{N \times N}$ are square matrices. They are formulated in the following ways:

$$\mathbf{A}_{ij} = \begin{cases} 1, & (v_i, v_j) \in \mathcal{E}; \\ 0, & (v_i, v_j) \notin \mathcal{E}, \end{cases} \quad (7)$$

and

$$\mathbf{D}_{ij} = \begin{cases} \sum_j \mathbf{A}_{ij}, & i = j; \\ 0, & i \neq j. \end{cases} \quad (8)$$

For the adjacency matrix \mathbf{A} , if node v_i and node v_j are connected, the corresponding element \mathbf{A}_{ij} is set to 1. Otherwise, \mathbf{A}_{ij} is 0 meaning node v_i and v_j are not connected.

The degree matrix \mathbf{D} is a diagonal matrix whose diagonal elements are the row sum of the corresponding rows of the adjacency matrix \mathbf{A} .

Based on the basic knowledge about the graph, the graph propagation mechanism can be described as follows. For each target node v_i , the information (i.e., node features) in the neighborhood of v_i , which is denoted as $N(v_i)$, is transformed, aggregated and combined with the transformed information of v_i to update the node features of v_i . Suppose the information transformation function is $f(\cdot)$ and the aggregation function is $\text{AGG}(\cdot)$. The iterative node feature aggregation and update process can be depicted in the formula below:

$$\mathbf{h}_i^{(l)} = \text{AGG}^{(l)}(\{f^{(l)}(\mathbf{h}_j^{(l-1)}), v_j \in N(v_i)\}, f^{(l)}(\mathbf{h}_i^{(l-1)})), \quad (9)$$

where $\mathbf{h}_i^{(0)}$ and $\mathbf{h}_j^{(0)}$ are the original node features \mathbf{x}_i and \mathbf{x}_j , respectively. In the GNN settings, the aggregation function and the information transformation function are linear or nonlinear transformations, which can be written as a combination of matrices and activation functions. The information transformation is conducted on node features individually, while aggregation is performed by merging information according to node neighborhood, which is defined by the adjacency matrix. Particularly, the aggregation operation must be invariant to node permutation. A simple example is formulated below.

$$\mathbf{H}^{(l+1)} = \sigma(\mathbf{A}\mathbf{H}^{(l)}\mathbf{W}^{(l)}), \quad (10)$$

where $\mathbf{H}^{(0)}$ is the original node features \mathbf{X} , $\sigma(\cdot)$ and $\mathbf{W}^{(l)}$ transform the information in nonlinear and linear manners, respectively, and the aggregation function is simply the summation among neighbor nodes.

4.2 RV Data Handling for Uncommon Trading Days

In order to leverage the data on both common trading days and uncommon trading days, special masks should be designed to identify inactive and active markets at each trading day. These masks should be applied to the input matrix, original node features \mathbf{X} , the

future RV data matrix \mathbf{Y} , and the adjacency matrix \mathbf{A} . Given the task of the DCRNN-RV model is to forecast future RV based on historical RV, each node only has a scalar feature, the historical RV value, at each trading day. However, for the uncommon trading days, there are missing RV values of the inactive markets. This gives rise to the first mask at the data processing level.

Here, the multivariate RV data are arranged in tables where row indices are the dates of observations and column indices are the chosen stock market indices. The notation is slightly different from the previous sections. Suppose the input RV data $\mathbf{X} \in \mathbb{R}^{T_X \times N}$ records the RV values for the union of trading days of all N stock market indices within a given look-back window, which means there are T_X RV values recorded for each stock market index in \mathbf{X} . In addition, the output RV data $\mathbf{Y} \in \mathbb{R}^{T_Y \times N}$ records the RV values for the union of trading days of all N stock market indices within a given forecast window, which means there are T_Y RV values recorded for each stock market index in \mathbf{Y} . Besides, \mathbf{Y} should be continuous with and succeeding \mathbf{X} in terms of time so that the row index of \mathbf{Y} starts with $T_X + 1$ and the total number of trading days T is calculated as $T = T_X + T_Y$. In each column of \mathbf{X} and \mathbf{Y} , there are some empty entries due to the trading dates difference in N distinct stock markets. Here, unless otherwise stated, the row index for dates is denoted by t and the column index for stock market indices is denoted by n , where $t \in \{1, 2, \dots, T\}$ and $n \in \{1, 2, \dots, N\}$. Hence, mask matrices $\mathbf{E}^X \in \mathbb{R}^{T_X \times N}$ and $\mathbf{E}^Y \in \mathbb{R}^{T_Y \times N}$ are constructed to handle missing values within \mathbf{X} and \mathbf{Y} , respectively. The two masks are formulated as below,

$$1 \leq t \leq T_X : \mathbf{E}_{tn}^X = \begin{cases} 0, & \mathbf{X}_{tn} \text{ is missing;} \\ 1, & \mathbf{X}_{tn} \text{ exists,} \end{cases} \quad (11)$$

and

$$T_X + 1 \leq t \leq T : \mathbf{E}_{tn}^Y = \begin{cases} 0, & \mathbf{Y}_{tn} \text{ is missing;} \\ 1, & \mathbf{Y}_{tn} \text{ exists.} \end{cases} \quad (12)$$

The masks \mathbf{E}^X and \mathbf{E}^Y are equivalent to filling the missing values with 0 at the data processing stage. However, these masks are essential in that the RV data are standardized before being processed by the DCRNN-RV model. After standardization, the filled 0 values become nonzero and values around the mean become very close to 0. It is difficult for the model to automatically capture the idea of active and inactive markets based on standardized data during training. However, these masks can remember the distribution of active and inactive markets for each day. Hence, the data used for model training becomes $\tilde{\mathbf{X}} = \mathbf{E}^X \odot \mathbf{X}$ and $\tilde{\mathbf{Y}} = \mathbf{E}^Y \odot \mathbf{Y}$, where \odot represents the element-wise multiplication between the two matrices. It is obvious that \mathbf{E}^X is important because it has to be applied to the data fed into the DCRNN-RV model.

On the other hand, in practice, stock exchanges in different markets release public holiday calendars annually which inform all scheduled market closures. Additionally, they may temporarily halt trading or adjust trading hours due to extraordinary events or policy changes, with advance notice to allow market participants to react accordingly. Although unscheduled halts are unpredictable, scheduled closures and policy changes are typically communicated well in advance. Hence, it is feasible to assume that stock market participants can know in advance when some of the markets are not active due to holidays or policies, while others remain active in the forecast period. In this way, \mathbf{E}^Y may not be useful with respect to forecast generation as stock market participants can proactively ignore those meaningless forecast values on inactive trading days for some markets. However, when it comes to model training, this output mask is necessary not only in missing value imputation for the target RV data, but also in loss calculation because it can ensure that the forecast on inactive markets does not affect the values of the trainable parameters through backward propagation. Here, the Mean Absolute Error (MAE) is used to measure the performance of the model during training, the loss calculation is performed as follows,

$$L = \frac{\sum_{t,n} |\tilde{\mathbf{Y}} - \mathbf{E}^Y \odot \hat{\mathbf{Y}}|}{\sum_{t,n} \mathbf{E}^Y}, \quad (13)$$

where $\widehat{\mathbf{Y}}$ is the forecast RV values produced by the DCRNN-RV model. The performance is measured only when relevant markets are active.

In addition to the two masks \mathbf{E}^X and \mathbf{E}^Y , another mask is designed and applied to the adjacency matrix \mathbf{A} to cut the connection between active markets and inactive markets. Here, for each $t \in T$, one corresponding adjacency mask should be constructed in the following way. The adjacency mask is denoted as $\mathbf{E}^{A_t} \in \mathbb{R}^{N \times N}$. Its elements in both the n^{th} row and the n^{th} column are set to 0 if $\tilde{\mathbf{X}}_{tn} = 0$ or $\tilde{\mathbf{Y}}_{tn} = 0$, where $\tilde{\mathbf{X}} = \mathbf{E}^X \odot \mathbf{X}$ and $\tilde{\mathbf{Y}} = \mathbf{E}^Y \odot \mathbf{Y}$. On the other hand, when $\tilde{\mathbf{X}}_{tn} \neq 0$ or $\tilde{\mathbf{Y}}_{tn} \neq 0$, elements in both the n^{th} row and the n^{th} column of \mathbf{E}^{A_t} are 1. Thus,

$$\forall k \in \{1, 2, \dots, N\}, \mathbf{E}_{nk}^{A_t} = \begin{cases} 0, & \text{if } \tilde{\mathbf{X}}_{tn} = 0 \text{ or } \tilde{\mathbf{Y}}_{tn} = 0; \\ 1, & \text{if } \tilde{\mathbf{X}}_{tn} \neq 0 \text{ or } \tilde{\mathbf{Y}}_{tn} \neq 0, \end{cases} \quad (14)$$

and

$$\forall k \in \{1, 2, \dots, N\}, \mathbf{E}_{kn}^{A_t} = \begin{cases} 0, & \text{if } \tilde{\mathbf{X}}_{tn} = 0 \text{ or } \tilde{\mathbf{Y}}_{tn} = 0; \\ 1, & \text{if } \tilde{\mathbf{X}}_{tn} \neq 0 \text{ or } \tilde{\mathbf{Y}}_{tn} \neq 0, \end{cases} \quad (15)$$

where $1 \leq n, k \leq N$ and $t \in \{1, 2, \dots, T\}$. As a result, a unique masked adjacency is constructed for each t : $\tilde{\mathbf{A}}_t = \mathbf{E}^{A_t} \odot \mathbf{A}$, where \mathbf{A} is the adjacency matrix for the whole T period. Although these masks are simple and straightforward, they are important to ensure that, during the training process, the inactive markets do not affect those active markets and vice versa.

4.3 Changing Graph Structure

In order to test whether a changing interrelationship pattern better captures the volatility dynamics for multiple stock markets and benefits multivariate RV forecast or not, the volatility relationship graph structures should be constructed prior to model training. Although learning the relationships among stock markets during training may contribute to a purely data-driven model such as V HAR-RV (equation (3)) and HAR-RV-KS (equa-

tion (4)), the estimated volatility network may deviate from reality given the limited expressiveness and flexibility of the model. However, for powerful models such as neural networks, formulating the interactions and interrelationships among variables during training can be too costly. Hence, injecting a prespecified graph structure into the model not only brings exogenous power to the model, but also accelerates the training process. This is also the reason that GNNs are preferred in this research.

For the DCRNN-RV model, volatility graphs are constructed by the DY framework (Diebold and Yilmaz, 2012). Suppose a multivariate time series $\{\mathbf{u}_t \in \mathbb{R}^N\}_{t=1}^T$ has N variables and it is covariance stationary. For this time series, a p -lag vector autoregression (VAR(p)) can be formulated as:

$$\mathbf{u}_t = \sum_{i=1}^p \phi_i \mathbf{u}_{t-i} + \boldsymbol{\epsilon}_t, \boldsymbol{\epsilon}_t \sim (0, \boldsymbol{\Sigma}_\epsilon), \quad (16)$$

where each ϕ_i is a scalar. The equation above can be reformulated in the moving average format:

$$\mathbf{u}_t = \sum_{i=1}^{\infty} \mathbf{B}_i \boldsymbol{\epsilon}_{t-i}, \quad (17)$$

where $\mathbf{B}_i = \sum_{j=1}^p \phi_j \mathbf{B}_{i-j}$. Here, $\mathbf{B}_0 = \mathbf{I}_{N \times N}$ and $\mathbf{B}_i = 0$ if $i < 0$. Through the variance decomposition of the H -step-ahead forecast error, the resulting matrix $\boldsymbol{\theta}^g(H)$ is derived and shown below.

$$\boldsymbol{\theta}_{ij}^g(H) = \frac{\sigma_{jj}^{-1} \sum_{h=0}^{H-1} (\mathbf{e}_i' \mathbf{B}_h \boldsymbol{\Sigma}_\epsilon \mathbf{e}_j)^2}{\sum_{h=0}^{H-1} (\mathbf{e}_i' \mathbf{B}_h \boldsymbol{\Sigma}_\epsilon \mathbf{B}_h' \mathbf{e}_i)}. \quad (18)$$

Here, \mathbf{e}_i is a selection vector with its i_{th} elements equal to 1 and 0 elsewhere. The matrix $\boldsymbol{\theta}^g(H)$ can be further standardized so that the row sum of the standardized matrix $\tilde{\boldsymbol{\theta}}^g(H)$ is 1,

$$\tilde{\boldsymbol{\theta}}_{ij}^g(H) = \frac{\boldsymbol{\theta}_{ij}^g(H)}{\sum_{j=1}^N \boldsymbol{\theta}_{ij}^g(H)}. \quad (19)$$

More details can be found in the original paper of the DY framework (Diebold and Yilmaz, 2012).

For this research, the standardized matrix $\tilde{\theta}^g(H)$ is considered as the adjacency matrix of the volatility interrelationship graph. In order to obtain the changing graph structure, for each training batch, the standardized matrix $\tilde{\theta}^g(H)$ is calculated based on the batch input data \mathbf{X} . In contrast to the study conducted by [Son et al. \(2023\)](#), this research does not further process the standardized matrix $\tilde{\theta}^g(H)$ nor use the net pairwise spillovers due to information preservation. However, to introduce some sparsity to the adjacency matrix, a certain proportion of the less significant edges is eliminated. This design not only saves the information on the volatility connection among markets, but also enhances the flexibility of the model because the sparsity of the connection can be adjusted. This means the connectivity between any two markets is bidirectional, if the impact in each direction is sufficiently significant.

[Son et al. \(2023\)](#) empirically proved that the DY framework can better capture the volatility interrelationship among stock market indices compared to the Pearson correlation coefficient. However, in practice, to apply the DY framework and to construct a dynamic graph adjacency matrix changing with respect to the input data \mathbf{X} for each training batch under the DY framework, the requirement is that the length of the input data, T_X , should be large enough to avoid numerical error. Hence, although the traditional HAR-RV (equation (2)) class of the model limit the time span of the input data to 22 days and achieves some good results under its simple architecture, this time span limitation is not suitable for the model proposed by this research for the sake of higher forecasting accuracy. In addition, volatility is persistent and has long-term memory, which gives an additional motivation to include more observations in the input data ([Poon and Granger, 2003](#)).

4.4 Proposed Model Formulation

Targeting traffic flow forecast, the DCRNN model applies diffusion convolution to process graphical information, which is transformed to formulate the gate units in its recurrent design ([Li et al., 2018](#)). For a given graph $\mathcal{G} = (\mathcal{V}, \mathcal{E})$ with its adjacency matrix \mathbf{A}

(equation (7)) and degree matrix \mathbf{D} (equation (8)), the diffusion process, which can capture the dynamics of the nodes in \mathcal{V} , is depicted by a random walk process on \mathcal{G} with restart probability $p \in [0, 1]$. For the random walk process, the state transition matrix can be calculated as $\mathbf{D}^{-1}\mathbf{A}$. It is the normalized adjacency matrix whose row sum equals 1 and each element $(\mathbf{D}^{-1}\mathbf{A})_{ij}$ denotes the probability from node (state) v_i to node (state) v_j . The random walk stochastic process can achieve stationarity after many transition iterations. The stationary distribution is denoted as $\mathbf{P} \in \mathbf{R}^{N \times N}$ whose elements \mathbf{P}_{ij} represents the probability of the diffusion process from node v_i to node v_j after numerous transition iterations. The close form of the stationary distribution \mathbf{P} is formulated below:

$$\mathbf{P} = \sum_{k=0}^{\infty} p(1-p)^k (\mathbf{D}^{-1}\mathbf{A}). \quad (20)$$

As a result, the diffusion convolution operation for node features (i.e., graph signals) $\mathbf{X} \in \mathbf{R}^N$ and the corresponding filter f_{θ} is formulated as:

$$\mathbf{X} *_G f_{\theta} = \sum_{k=0}^{K-1} \theta_k (\mathbf{D}^{-1}\mathbf{A})^k \mathbf{X}, \quad (21)$$

where θ_k is the trainable parameters and K is the parameter to control the receptive field of the graph information propagation through the diffusion convolution operation. The original DCRNN model also uses the reverse diffusion process. However, given the adjacency matrix is constructed under the DY framework, the pairwise volatility spillover effect is already bidirectional, thus eliminating the need to include the reverse diffusion process.

Based on the diffusion convolution operation, the temporal dynamics of the nodes are modelled through the Gated Recurrent Units (GRU) (Chung et al., 2014), which is an effective variant of RNNs. In the DCRNN model, the Diffusion Convolutional Gated Recurrent Unit (DCGRU) is formulated using the current node features $\mathbf{X}^{(t)}$ at time t and the previous hidden state $\mathbf{H}^{(t-1)}$ to update the information carried by the hidden

states $\mathbf{H}^{(t)}$ through the reset gate $\mathbf{r}^{(t)}$ and update gate $\mathbf{u}^{(t)}$ at time t .

$$\begin{aligned}
\mathbf{r}^{(t)} &= \sigma_{\text{GRU}}(\boldsymbol{\theta}_r *_{\mathcal{G}} [\mathbf{X}^{(t)}, \mathbf{H}^{(t-1)}] + \mathbf{b}_r), \\
\mathbf{u}^{(t)} &= \sigma_{\text{GRU}}(\boldsymbol{\theta}_u *_{\mathcal{G}} [\mathbf{X}^{(t)}, \mathbf{H}^{(t-1)}] + \mathbf{b}_u), \\
\mathbf{C}^{(t)} &= \tanh(\boldsymbol{\theta}_C *_{\mathcal{G}} [\mathbf{X}^{(t)}, (\mathbf{r}^{(t)} \odot \mathbf{H}^{(t-1)})] + \mathbf{b}_C), \\
\mathbf{H}^{(t)} &= \mathbf{u}^{(t)} \odot \mathbf{H}^{(t-1)} + (1 - \mathbf{u}^{(t)}) \odot \mathbf{C}^{(t)},
\end{aligned} \tag{22}$$

where $*_{\mathcal{G}}$ is the graph diffusion convolution defined in equation (21) and θ_r , θ_u and θ_C are the trainable parameters of the relevant filters.

Different from the traditional HAR-RV class of models, the DCRNN model can perform a multi-step ahead forecast directly instead of repeating the one-step ahead forecast. The multi-step ahead forecast function is realized through the Sequence to Sequence (Seq2Seq) architecture proposed by Sutskever et al. (2014). This architecture employs encoders and decoders, which are both formulated as equation (22). The final output hidden state of the encoders is passed to the decoders as the initial hidden state to generate forecasts sequentially.

An overview of the whole DCRNN model is provided in Figure 1 below:

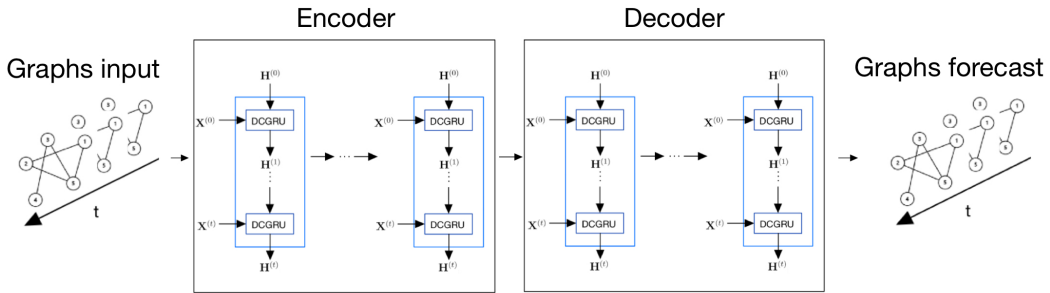


Figure 1: An overview of the DCRNN model (Li et al., 2018)

In the context of the dynamic RV forecast, the encoders encode the RV information in the look-back input window, \mathbf{X} , whereas the decoders generate the forecast, \hat{Y} . The diffusion convolution operation of encoders and decoders can be formulated as follows:

For encoders

$$\tilde{\mathbf{X}}_{t,:} *_{\mathcal{G}} f_{\theta} = \sum_{k=0}^{K-1} \theta_k (\tilde{\mathbf{D}}_t^{-1} \tilde{\mathbf{A}}_t)^k \tilde{\mathbf{X}}_{t,:}, \quad (23)$$

and for decoders

$$\tilde{\mathbf{Y}}_{t,:} *_{\mathcal{G}} f_{\theta} = \sum_{k=0}^{K-1} \theta_k (\tilde{\mathbf{D}}_t^{-1} \tilde{\mathbf{A}}_t)^k \tilde{\mathbf{Y}}_{t,:}, \quad (24)$$

where $\tilde{\mathbf{X}}_{t,:}$ is the t^{th} row of $\mathbf{E}^X \odot \mathbf{X}$ (equation (11)) and $\tilde{\mathbf{Y}}_{t,:}$ is the t^{th} row of $\mathbf{E}^Y \odot \mathbf{Y}$ (equation (12)). Besides, $\tilde{\mathbf{A}}_t = \mathbf{E}^{A_t} \odot \mathbf{A}$ with \mathbf{E}^{A_t} formulated as either equation (14) or equation (15) and $\tilde{\mathbf{D}}_t$ is the corresponding degree matrix of the masked adjacency matrix $\tilde{\mathbf{A}}_t$. For neural network batch training architecture, each training batch consists of data pairs of consecutive input and target RV values $\{(\tilde{\mathbf{X}}, \tilde{\mathbf{Y}})\}_{i=0}^B$, where B is the batch size. Hence, for each $\tilde{\mathbf{X}}$ and $\tilde{\mathbf{Y}}$ pair, an adjacency matrix \mathbf{A} is formulated based on the common trading days observations in the input data \mathbf{X} under the DY Framework, which aims to avoid the influence from the imputed value to the volatility network structure. On the other hand, $T_X \times B$ and $T_Y \times B$ adjacency matrix masks \mathbf{E}^{A_t} have to be constructed and attached to the data loaders to calculate the masked adjacency matrix $\tilde{\mathbf{A}}_t$ for each row of the $\tilde{\mathbf{X}}$ and $\tilde{\mathbf{Y}}$.

5 Experiments

This section empirically evaluates the performance of the proposed DCRNN-RV model, based on the chosen datasets. The experiments involve comparing the DCRNN-RV model and baseline models to determine the power of the DCRNN-RV model and to empirically discover new insights towards the dynamics of RV.

5.1 Model Evaluation Tools

To better assess the effectiveness of the DCRNN-RV model, various evaluation criteria are involved. MAE is used to measure the training and testing errors of the direct forecast of different models. In addition, the output series generated by different models through the iterated forecast method are compared. For model training and testing, forecasts \mathbf{Y}

are always generated based on real data input $\tilde{\mathbf{X}}$. However, under the iterated forecast framework, the output forecast RV values from the model are used as the RV input to generate further RV forecasts. Compared to direct forecast, the iterated forecast method carries and aggregates the randomness or error in previous forecasts, which amplifies the impact from the quality of the model to the whole forecast series. Once the iterated forecast series of all stock market indices are obtained for different models, the Mean Absolute Forecast Error (MAFE) is used to evaluate the quality of the series for each stock market index due to its robustness (Hansen and Lunde, 2005). Besides, the Diebold-Mariano (DM) test (Diebold and Mariano, 2002; Harvey et al., 1997) and the Model Confidence Set (MCS) test (Hansen et al., 2011) are used to compare whether the iterated forecast series produced by one model are significantly better than those generated by another on an index-wise basis.

In the out-of-sample forecast analysis, multiple forecasting windows are applied: $h = 1, 5, 10, 22$, which represents the short-term (daily), mid-term (weekly) and long-term (monthly) forecasting. In addition, the look-back window, the time window of the in-sample data, is chosen to be 100, 250 and 500, which approximately represents the historical time window for 6 months (short-term window), 12 months (mid-term window) and 24 months (long-term window), respectively. The length of the look-back window is denoted as l . For models such as the proposed DCRNN-RV and the STG-Spillover model designed by Son et al. (2023), they are capable of generating direct forecasts for each of the forecasting windows through the Seq2Seq architecture. Hence, these models are independently trained and generate iterative forecast series for different combinations of the look-back window l and the forecast window h so that their expressiveness can be fully evaluated under different settings.

The hardware and software configurations are:

- Operating system: Windows 11
- CPU: 13th Gen Intel(R) Core(TM) i9-13900HX

- GPU: NVIDIA GeForce RTX 4080 Laptop GPU
- Software: Python 3.10.14; NumPy 1.26.4; PyTorch 1.13.1+cu116; PyTorch Geometric 2.3.1

5.2 Benchmark Datasets and Baseline models

The benchmark datasets consist of the square root of RV data of eight stock market indices. These indices are from both markets that are known to be influential and those that are not. The indices are SPX (US), GDAXI (Germany), FCHI (France), FTSE (UK), OMXSPI (Sweden), N225 (Japan), KS11 (South Korea) and HSI (Hong Kong), which are often used in RV forecast studies (e.g., (Liang et al., 2020), (Son et al., 2023)). The RV is calculated based on the 5-minute high-frequency returns. The dataset includes the union of the trading days of the eight stock markets from October 2006 to June 2022, which is 4079 trading days in total.

The descriptive analysis of the square-rooted data for each market index is reported in the table below (Table 1). The Augmented Dickey-Fuller (ADF) test (MacKinnon, 1994; Cheung and Lai, 1995) is also conducted to reject, at the 5% confidence level, the null hypothesis that a unit root exists in the square-rooted RV series of each stock market index as the p-values are less than 5%. This indicates that each square-rooted RV series is stationary. Besides, in Figure 2, the square-rooted RV series of each stock market index is visualized with grey, yellow and red areas indicating the Global Financial Crisis period, European Sovereign Debt Crisis period, and COVID-19 Pandemic period, respectively.

| Index | Mean | Standard Deviation | Skewness | Kurtosis | ADF Statistic | ADF p-value |
|---------|---------|--------------------|----------|----------|---------------|-------------|
| .SPX | 0.00838 | 0.0067 | 3.40055 | 18.74163 | -7.17866 | 0.0 |
| .GDAXI | 0.00967 | 0.00596 | 3.26407 | 19.1322 | -5.67368 | 0.0 |
| .FCHI | 0.00973 | 0.00587 | 3.14475 | 18.10663 | -5.91484 | 0.0 |
| .FTSE | 0.00931 | 0.00631 | 4.00029 | 30.77746 | -7.24441 | 0.0 |
| .OMXSPI | 0.00822 | 0.00599 | 4.52456 | 39.25867 | -5.22361 | 0.00001 |
| .N225 | 0.0082 | 0.00512 | 3.48436 | 19.75396 | -7.60245 | 0.0 |
| .KS11 | 0.00768 | 0.00505 | 4.19736 | 29.89983 | -6.63205 | 0.0 |
| .HSI | 0.00859 | 0.00483 | 3.5094 | 21.62236 | -4.66039 | 0.0001 |

Table 1: Descriptive statistics of the square-rooted RV data.

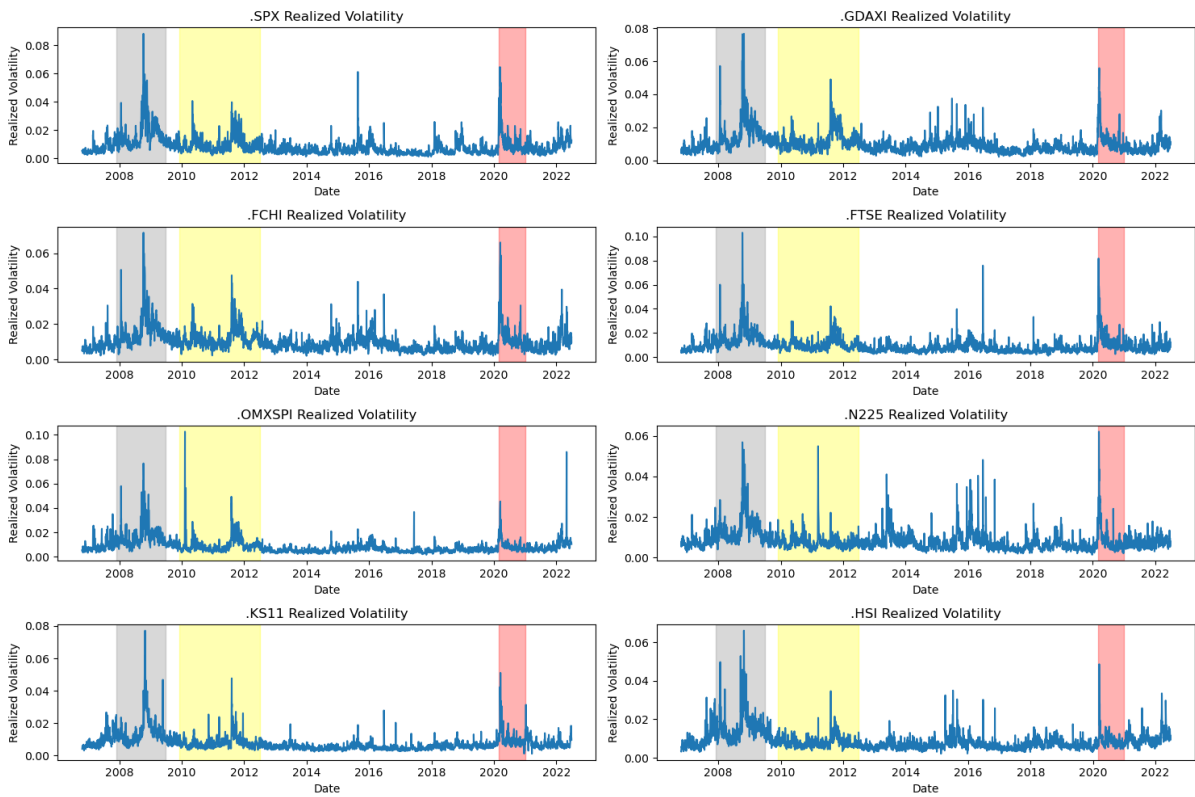


Figure 2: Visualization of the square-rooted RV series of each stock market index

In addition, the net volatility spillover effect is measured under the DY framework for each stock market index and presented in Table 2. A positive net volatility spillover effect indicates that a stock market transmits more volatility to other stock markets than it receives from them. On the other hand, a negative net volatility spillover effect indicates that a stock market receives more volatility from other stock markets than it transmits to them. Hence, the SPX, FCHI, FTSE and GDAXI are the influential stock markets and the HSI, OMXSPI, KS11 and N225 are the impressionable or susceptible stock markets.

| Stock Market Index | Net Volatility Spillover Effect |
|--------------------|---------------------------------|
| SPX | 9.2959 |
| FCHI | 4.3617 |
| FTSE | 3.0469 |
| HSI | -7.15892 |
| OMXSPI | -2.4636 |
| KS11 | -5.93717 |
| GDAXI | 3.88085 |
| N225 | -5.0256 |

Table 2: The net volatility spillover effect measured under the DY framework

Since this research focuses on improving the existing DCRNN-based model for RV forecast proposed by Son et al. (2023), the baseline model is the STG-Spillover model. Although the values of the hyperparameters and the exact construction of the model are not available, both the improved DCRNN-RV and the original STG-Spillover models for RV forecast in this research are constructed based on the initial DCRNN research from Li et al. (2018). To ensure the fairness of the experiment, all hyperparameters for the DCRNN-RV model and STG-Spillover model are equal. The RV dataset used in the experiment, the code of the experiment and the relevant hyperparameter settings can be found at <https://github.com/MikeZChi/DCRNN-RV.git>.

5.3 Experiment Results

The MAE scores for the direct forecast generated by the tested models on out-sample data under different forecast settings are listed in Tables 3, 4 and 5 below. The smaller MAE scores are bolded and can be regarded as better forecast performances. From the results, it can be concluded that the proposed DCRNN-RV model is superior to the STG-Spillover model for all different look-back window and forecast window combinations.

| MAE ($l = 100$) | $h = 1$ | $h = 5$ | $h = 10$ | $h = 22$ |
|-------------------|----------------|---------------|----------------|----------------|
| DCRNN-RV | 0.00243 | 0.0028 | 0.00277 | 0.00297 |
| STG-Spillover | 0.00274 | 0.00292 | 0.00337 | 0.00352 |

Table 3: The MAE scores for the tested models with a 6-month look-back window. Smaller MAE losses are bolded.

| MAE ($l = 250$) | $h = 1$ | $h = 5$ | $h = 10$ | $h = 22$ |
|--------------------------|---------------|----------------|----------------|----------------|
| DCRNN-RV | 0.0024 | 0.00252 | 0.00285 | 0.00306 |
| STG-Spillover | 0.00283 | 0.00296 | 0.00313 | 0.00361 |

Table 4: The MAE scores for the tested models with a 12-month look-back window. Smaller MAE losses are bolded.

| MAE ($l = 500$) | $h = 1$ | $h = 5$ | $h = 10$ | $h = 22$ |
|--------------------------|----------------|----------------|----------------|----------------|
| DCRNN-RV | 0.00232 | 0.00265 | 0.00285 | 0.00326 |
| STG-Spillover | 0.00272 | 0.00303 | 0.00337 | 0.0034 |

Table 5: The MAE scores for the tested models with a 24-month look-back window. Smaller MAE losses are bolded.

However, as mentioned earlier, in the MAE test, forecasts are produced based on the real data in the look-back window. This is different from the iterated forecast method, where forecasts are produced based on the look-back window data that are derived from previous forecasts. Besides, it is hard to tell whether one model is actually significantly better than the other one or whether one model performs better only in certain markets instead of all markets based on the MAE loss comparison tables. Hence, further tests are conducted in an iterated forecast manner.

Based on the iterated forecast RV series for each market, the MAFE loss is calculated as follows:

$$\text{MAFE}_i^{(h)} = \frac{1}{T_{\text{test}} - h + 1} \sum_{t=0}^{T_{\text{test}}-h} |\widehat{\text{RV}}_{i,t+h}^{\frac{1}{2}} - \text{RV}_{i,t+h}^{\frac{1}{2}}|, \quad (25)$$

where T_{test} denotes the duration in time of the test dataset and h is the forecast window. The MAFE loss of the iterated forecast RV series for each market generated by the two models with different (l, h) pairs are presented in the tables below.

| MAFE ($l = 100$) | $h = 1$ | | $h = 5$ | |
|--------------------|----------------|----------------|----------------|----------------|
| | DCRNN-RV | STG-Spillover | DCRNN-RV | STG-Spillover |
| SPX | 0.00376 | 0.00385 | 0.00364 | 0.00413 |
| FCHI | 0.00384 | 0.00565 | 0.00354 | 0.00441 |
| FTSE | 0.00333 | 0.00341 | 0.00339 | 0.0036 |
| HSI | 0.00302 | 0.0028 | 0.00239 | 0.00236 |
| OMXSPI | 0.00233 | 0.00263 | 0.00235 | 0.00264 |
| KS11 | 0.00218 | 0.00278 | 0.00223 | 0.00232 |
| GDAXI | 0.00284 | 0.0034 | 0.00295 | 0.00329 |
| N225 | 0.00238 | 0.0027 | 0.00235 | 0.00269 |
| MAFE ($l = 100$) | $h = 10$ | | $h = 22$ | |
| | DCRNN-RV | STG-Spillover | DCRNN-RV | STG-Spillover |
| SPX | 0.0036 | 0.00422 | 0.00377 | 0.00466 |
| FCHI | 0.00364 | 0.00418 | 0.00341 | 0.00433 |
| FTSE | 0.00333 | 0.00383 | 0.00349 | 0.00404 |
| HSI | 0.00272 | 0.00268 | 0.00213 | 0.00218 |
| OMXSPI | 0.00234 | 0.00314 | 0.00233 | 0.0027 |
| KS11 | 0.00287 | 0.00258 | 0.00206 | 0.00253 |
| GDAXI | 0.00295 | 0.0037 | 0.00286 | 0.00342 |
| N225 | 0.00236 | 0.00261 | 0.0025 | 0.00243 |

Table 6: The table includes the MAFE loss for each stock market index with a 6-month look-back window. Smaller MAFE losses are bolded.

| MAFE ($l = 250$) | $h = 1$ | | $h = 5$ | |
|--------------------|----------------|----------------|----------------|----------------|
| | DCRNN-RV | STG-Spillover | DCRNN-RV | STG-Spillover |
| SPX | 0.00407 | 0.00639 | 0.00375 | 0.00403 |
| FCHI | 0.00363 | 0.00596 | 0.00355 | 0.00537 |
| FTSE | 0.00371 | 0.00429 | 0.00355 | 0.00372 |
| HSI | 0.00296 | 0.00371 | 0.00247 | 0.00247 |
| OMXSPI | 0.00275 | 0.00311 | 0.00251 | 0.00268 |
| KS11 | 0.00235 | 0.00232 | 0.00217 | 0.0025 |
| GDAXI | 0.00299 | 0.00365 | 0.00307 | 0.00341 |
| N225 | 0.00244 | 0.00263 | 0.0024 | 0.00248 |
| MAFE ($l = 250$) | $h = 10$ | | $h = 22$ | |
| | DCRNN-RV | STG-Spillover | DCRNN-RV | STG-Spillover |
| SPX | 0.00383 | 0.00504 | 0.00375 | 0.00491 |
| FCHI | 0.0043 | 0.00653 | 0.00392 | 0.00432 |
| FTSE | 0.00371 | 0.00402 | 0.00368 | 0.00402 |
| HSI | 0.00306 | 0.00323 | 0.0025 | 0.00241 |
| OMXSPI | 0.00256 | 0.00301 | 0.00274 | 0.00297 |
| KS11 | 0.0024 | 0.00234 | 0.0028 | 0.00248 |
| GDAXI | 0.00351 | 0.00642 | 0.00337 | 0.0066 |
| N225 | 0.00252 | 0.00255 | 0.00238 | 0.00243 |

Table 7: The table includes the MAFE loss for each stock market index with a 12-month look-back window. Smaller MAFE losses are bolded.

| MAFE ($l = 500$) | $h = 1$ | | $h = 5$ | |
|--------------------|----------------|----------------|----------------|----------------|
| | DCRNN-RV | STG-Spillover | DCRNN-RV | STG-Spillover |
| SPX | 0.00433 | 0.0043 | 0.00419 | 0.00419 |
| FCHI | 0.00428 | 0.00702 | 0.00414 | 0.0043 |
| FTSE | 0.00399 | 0.00609 | 0.00405 | 0.00429 |
| HSI | 0.00293 | 0.00346 | 0.00298 | 0.00274 |
| OMXSPI | 0.00296 | 0.00351 | 0.00282 | 0.00299 |
| KS11 | 0.00276 | 0.00317 | 0.00282 | 0.0029 |
| GDAXI | 0.00349 | 0.00365 | 0.00347 | 0.00364 |
| N225 | 0.00266 | 0.00281 | 0.00254 | 0.003 |
| MAFE ($l = 500$) | $h = 10$ | | $h = 22$ | |
| | DCRNN-RV | STG-Spillover | DCRNN-RV | STG-Spillover |
| SPX | 0.0041 | 0.00508 | 0.00413 | 0.00437 |
| FCHI | 0.00408 | 0.0054 | 0.00414 | 0.00575 |
| FTSE | 0.00418 | 0.00494 | 0.00409 | 0.00435 |
| HSI | 0.00295 | 0.00249 | 0.00266 | 0.00319 |
| OMXSPI | 0.00287 | 0.00333 | 0.0029 | 0.00377 |
| KS11 | 0.00257 | 0.00316 | 0.00248 | 0.00265 |
| GDAXI | 0.00335 | 0.00461 | 0.00353 | 0.0056 |
| N225 | 0.00262 | 0.00287 | 0.00265 | 0.00298 |

Table 8: The table includes the MAFE loss for each stock market index with a 24-month look-back window. Smaller MAFE losses are bolded.

According to Tables 6, 7 and 8, it is clear that, regardless of the different look-back and forecast window settings, the DCRNN-RV model always performs better in at least 6 out of 8 stock market indices compared to the STG-Spillover model. Based on the results of the MAFE loss, further tests are conducted to evaluate whether the superiority of the DCRNN-RV model over the STG-Spillover model in different markets is statistically significant.

The DM test is designed to compare the quality of two forecast series based on the differences between two series of forecast errors (Diebold and Mariano, 2002). Set the forecast errors of model 0 and model 1 as $\{e_{0,t}\}_{t=1}^T$ and $\{e_{1,t}\}_{t=1}^T$, respectively. Suppose function $g(\cdot)$ can be used to calculate the distance between the two series of forecast errors. Here, $g(\cdot)$ is set such that $g(e_{0,t}, e_{1,t}) = e_{0,t} - e_{1,t}$ and $e_{i,t}$ is the absolute error of model i ($i \in \{0, 1\}$) at time t : $e_{i,t} = |\widehat{RV}_{i,t} - RV_{i,t}|$ for all stock market indices. The test

statistic of the DM test, denoted as D , can be calculated as:

$$D = V_d^{-\frac{1}{2}} \bar{d}, \quad (26)$$

where V_d is the normalized, weighted sum of the lagged autocovariances of $\{d_t\}_{t=1}^T$, $\bar{d} = \frac{1}{T} \sum_{t=1}^T d_t$ and $d_t = g(e_{0,t}, e_{1,t}) = e_{0,t} - e_{1,t}$. From the formula, it is clear that, when D is a positive number, \bar{d} should also be positive because $V_d^{-\frac{1}{2}}$ is non-negative. If \bar{d} is positive, it means that, on average, the error from model 1, $\{e_{1,t}\}_{t=1}^T$, is less than the error from model 0, $\{e_{0,t}\}_{t=1}^T$. When D is sufficiently large, the DM test can conclude that model 1 produces a significantly more accurate forecast series than model 0. The results of the DM test can be found in Tables 9, 10 and 11. For each DM test, model 0 is the STG-Spillover model and model 1 is the DCRNN-RV model. The null hypothesis is that the DCRNN-RV model forecast is less or equally accurate compared to the STG-Spillover model forecast. If the test statistics D is sufficiently large and the p -value is less than the significance level α , the null hypothesis is rejected and the test results are in favor of the alternative hypothesis, which means the DCRNN-RV model forecast is more accurate than the STG-Spillover model forecast. Here, the significant level α is set to be 0.05.

| DM ($l = 100$) | $h = 1$ | | $h = 5$ | |
|------------------|----------------|-----------------|----------------|-----------------|
| | DM statistic | p-value | DM statistic | p-value |
| SPX | 0.90548 | 0.1827 | 2.6282 | 0.0435 |
| FCHI | 8.08585 | 7.77E-16 | 5.8727 | 2.82E-09 |
| FTSE | 1.6861 | 0.04602 | 2.93393 | 0.00171 |
| HSI | -3.19899 | 0.99929 | -0.18698 | 0.57415 |
| OMXSPI | 3.93832 | 6.54E-05 | 3.12315 | 0.00092 |
| KS11 | 5.74565 | 5.89E-09 | 0.46988 | 0.31927 |
| GDAXI | 5.36198 | 4.99E-08 | 2.84359 | 0.00227 |
| N225 | 2.10865 | 0.0176 | 2.8208 | 0.00244 |
| DM ($l = 100$) | $h = 10$ | | $h = 22$ | |
| | DM statistic | p-value | DM statistic | p-value |
| SPX | 3.34081 | 0.00043 | 3.1912 | 0.00073 |
| FCHI | 4.50592 | 3.65E-06 | 3.90542 | 4.98E-05 |
| FTSE | 3.66831 | 0.00013 | 4.93472 | 4.62E-07 |
| HSI | -0.27988 | 0.61019 | 0.39806 | 0.34533 |
| OMXSPI | 5.30571 | 6.78E-08 | 2.82266 | 0.00242 |
| KS11 | -1.10913 | 0.86619 | 3.19277 | 0.00072 |
| GDAXI | 5.64226 | 1.06E-08 | 2.84067 | 0.00229 |
| N225 | 2.26343 | 0.0119 | -1.14983 | 0.87477 |

Table 9: The DM test results table under a 6-month look-back window with significant results in bold at 5% level

| DM ($l = 250$) | $h = 1$ | | $h = 5$ | |
|------------------|----------------|-----------------|----------------|-----------------|
| | DM statistic | p-value | DM statistic | p-value |
| SPX | 3.7148 | 0.00011 | 2.48264 | 0.0066 |
| FCHI | 6.16187 | 5.26E-10 | 4.46286 | 4.51E-06 |
| FTSE | 2.47602 | 0.00673 | 2.24422 | 0.01252 |
| HSI | 8.70545 | 0 | -0.15212 | 0.56044 |
| OMXSPI | 1.49069 | 0.06818 | 0.94373 | 0.17277 |
| KS11 | -0.39431 | 0.65328 | 3.50849 | 0.00024 |
| GDAXI | 3.45029 | 0.00029 | 1.90508 | 0.02853 |
| N225 | 3.56156 | 0.00019 | 1.11351 | 0.13288 |
| DM ($l = 250$) | $h = 10$ | | $h = 22$ | |
| | DM statistic | p-value | DM statistic | p-value |
| SPX | 3.83623 | 6.65E-05 | 3.59874 | 0.00017 |
| FCHI | 6.46598 | 7.96E-11 | 3.53577 | 0.00021 |
| FTSE | 2.41136 | 0.00804 | 2.38887 | 0.00855 |
| HSI | 1.90022 | 0.02885 | -0.95103 | 0.82909 |
| OMXSPI | 4.39318 | 6.20E-06 | 2.58281 | 0.00497 |
| KS11 | -0.71659 | 0.7631 | -3.13219 | 0.99911 |
| GDAXI | 7.36862 | 1.84E-13 | 9.43949 | 0 |
| N225 | 0.3482 | 0.36388 | 0.662 | 0.25406 |

Table 10: The DM test results table under a 12-month look-back window with significant results in bold at 5% level

| DM ($l = 500$) | $h = 1$ | | $h = 5$ | |
|------------------|----------------|-----------------|----------------|-----------------|
| | DM statistic | p-value | DM statistic | p-value |
| SPX | -0.36511 | 0.64243 | 0.03603 | 0.48564 |
| FCHI | 4.80687 | 9.32E-07 | 2.50387 | 0.00625 |
| FTSE | 4.91783 | 5.42E-07 | 3.44336 | 0.0003 |
| HSI | 3.82212 | 7.19E-05 | -2.61245 | 0.99541 |
| OMXSPI | 3.65707 | 0.00014 | 2.46311 | 0.007 |
| KS11 | 1.61362 | 0.05352 | 1.31979 | 0.09366 |
| GDAXI | 2.47813 | 0.00672 | 2.79924 | 0.00263 |
| N225 | 2.11052 | 0.01758 | 3.94204 | 4.43E-05 |
| DM ($l = 500$) | $h = 10$ | | $h = 22$ | |
| | DM statistic | p-value | DM statistic | p-value |
| SPX | 3.17178 | 0.00079 | 1.7 | 0.04479 |
| FCHI | 4.98798 | 3.82E-07 | 3.74048 | 9.93E-05 |
| FTSE | 2.07903 | 0.01898 | 2.16915 | 0.0152 |
| HSI | -2.5339 | 0.99425 | 6.63498 | 3.24E-11 |
| OMXSPI | 2.08877 | 0.01854 | 3.15272 | 0.00084 |
| KS11 | 2.67661 | 0.0038 | 1.92678 | 0.027205 |
| GDAXI | 3.36045 | 0.0004 | 5.42859 | 3.91E-08 |
| N225 | 1.78315 | 0.03749 | 2.49074 | 0.00649 |

Table 11: The DM test results table under a 24-month look-back window with significant results in bold at 5% level

According to the DM test results in Tables 9, 10 and 11, the forecast series generated by the DCRNN-RV model always delivers significantly smaller absolute forecast error compared to that generated by the STG-Spillover model for a least 5 out of 8 stock market indices. Hence, it is feasible to conclude that, for the majority of stock market indices, the DCRNN-RV model forecast is more accurate compared to the STG-Spillover model forecast at 5% confidence level.

In addition to the DM test, the MCS test is conducted to verify the superiority of the DCRNN-RV model further. Proposed by Hansen et al. (2011), the MCS test is a statistical method used to evaluate the relative performance of a group of predictive models. The test systematically compares different models to identify a subset of models that are statistically indistinguishable in terms of their forecasting accuracy. By eliminating inferior models, the MCS test ensures that the remaining set of models performs best at a given confidence level. The MCS test results of the two models under different look-back and forecast window settings are reported in Tables 12, 13 and 14 at a 10% confidence

level.

| MCS | $h = 1$ | | $h = 5$ | |
|-------------|----------------|----------------|----------------|----------------|
| $(l = 100)$ | DCRNN-RV | STG-Spillover | DCRNN-RV | STG-Spillover |
| SPX | 1 | 0.31213 | 1 | 0.00443 |
| FCHI | 1 | 0 | 1 | 0 |
| FTSE | 1 | 0.09224 | 1 | 0 |
| HSI | 0.00203 | 1 | 0.83726 | 1 |
| OMXSPI | 1 | 0.0014 | 1 | 0.00137 |
| KS11 | 1 | 0 | 1 | 0.59615 |
| GDAXI | 1 | 0 | 1 | 0.00422 |
| N225 | 1 | 0.0165 | 1 | 0.00243 |
| MCS | $h = 10$ | | $h = 22$ | |
| $(l = 100)$ | DCRNN-RV | STG-Spillover | DCRNN-RV | STG-Spillover |
| SPX | 1 | 0 | 1 | 0.0011 |
| FCHI | 1 | 0 | 1 | 0.00131 |
| FTSE | 1 | 0.0012 | 1 | 0 |
| HSI | 0.74631 | 1 | 1 | 0.67426 |
| OMXSPI | 1 | 0 | 1 | 0.00142 |
| KS11 | 0.2282 | 1 | 1 | 0 |
| GDAXI | 1 | 0 | 1 | 0.0016 |
| N225 | 1 | 0.01516 | 0.2164 | 1 |

Table 12: The MCS test results table under a 6-month look-back window with bold representing model included in the MCS at 10% level

| MCS | $h = 1$ | | $h = 5$ | |
|-------------|----------------|----------------|----------------|----------------|
| $(l = 250)$ | DCRNN-RV | STG-Spillover | DCRNN-RV | STG-Spillover |
| SPX | 1 | 0 | 1 | 0.0063 |
| FCHI | 1 | 0 | 1 | 0 |
| FTSE | 1 | 0.0064 | 1 | 0.01865 |
| HSI | 1 | 0 | 0.87713 | 1 |
| OMXSPI | 1 | 0.12114 | 1 | 0.3124 |
| KS11 | 0.67241 | 1 | 1 | 0 |
| GDAXI | 1 | 0 | 1 | 0.0452 |
| N225 | 1 | 0 | 1 | 0.25413 |
| MCS | $h = 10$ | | $h = 22$ | |
| $(l = 250)$ | DCRNN-RV | STG-Spillover | DCRNN-RV | STG-Spillover |
| SPX | 1 | 0 | 1 | 0 |
| FCHI | 1 | 0 | 1 | 0.0013 |
| FTSE | 1 | 0.0106 | 1 | 0.00563 |
| HSI | 1 | 0.0458 | 0.3162 | 1 |
| OMXSPI | 1 | 0 | 1 | 0.00712 |
| KS11 | 0.43816 | 1 | 1 | 0.00115 |
| GDAXI | 1 | 0 | 1 | 0 |
| N225 | 1 | 0.71247 | 1 | 0.50225 |

Table 13: The MCS test results table under a 12-month look-back window with bold representing model included in the MCS at 10% level

| MCS | $h = 1$ | | $h = 5$ | |
|---------------|---------------|---------------|----------|----------------|
| ($l = 500$) | DCRNN-RV | STG-Spillover | DCRNN-RV | STG-Spillover |
| SPX | 0.7361 | 1 | 1 | 0.9692 |
| FCHI | 1 | 0 | 1 | 0.00431 |
| FTSE | 1 | 0 | 1 | 0 |
| HSI | 1 | 0 | 0.00511 | 1 |
| OMXSPI | 1 | 0 | 1 | 0.0124 |
| KS11 | 1 | 0.07308 | 1 | 0.19923 |
| GDAXI | 1 | 0.00835 | 1 | 0.00541 |
| N225 | 1 | 0.01847 | 1 | 0.00133 |
| MCS | $h = 10$ | | $h = 22$ | |
| ($l = 500$) | DCRNN-RV | STG-Spillover | DCRNN-RV | STG-Spillover |
| SPX | 1 | 0 | 1 | 0.07514 |
| FCHI | 1 | 0 | 1 | 0 |
| FTSE | 1 | 0.01932 | 1 | 0.01734 |
| HSI | 0.00623 | 1 | 1 | 0 |
| OMXSPI | 1 | 0.0221 | 1 | 0 |
| KS11 | 1 | 0.00241 | 1 | 0.03418 |
| GDAXI | 1 | 0 | 1 | 0 |
| N225 | 1 | 0.05817 | 1 | 0.01229 |

Table 14: The MCS test results table under a 24-month look-back window with bold representing model included in the MCS at 10% level

The MCS test results are similar to the DM test results. According to the MCS test, the DCRNN-RV model consistently remains in the MCS for at least 7 out of 8 stock market indices under various settings of the look-back and forecast windows. In contrast, the STG-Spillover model remains in the MCS much less frequently.

Based on the DM and MCS test results, when the DCRNN-RV model fails to yield significantly more accurate forecasts than the STG-Spillover model, it usually occurs for stock market indices HSI, KS11 and N225. This does not indicate the proposed DCRNN-RV model is worse than the STG-Spillover model in these markets. According to the MAFE results in Tables 6, 7 and 8, the DCRNN-RV model achieves lower MAFE results 6 times for the HSI index, 8 times for the KS11 index and 12 times for the N225 index out of the 12 experiments. The DCRNN-RV model achieves significantly better results compared to the STG-Spillover less frequently when forecasting HSI, KS11, and N225 than when forecasting other stock market indices. This might be attributed to HSI, KS11, and N225 being impressionable or susceptible stock markets as defined in Table 2. On the other

hand, although OMXSPI is also an impressionable stock market, the DCRNN-RV model performs exceptionally well when forecasting the RV for OMXSPI.

To explain this phenomenon, a scalar ω is calculated for each stock market index to measure how frequently a stock market is inactive with zero RV values on days when at least 5 other markets are otherwise active. According to Table 15, the ω values for HSI, KS11 and N225 are quite high compared to that for OMXSPI. The difference can be interpreted as follows. Given that the impressionable stock markets are more likely to be influenced by other markets compared to affected other markets, HSI, KS11 and N225 missed more opportunities to be influenced because they are often inactive when more than half of the stock markets are active. On the contrary, although OMXSPI is also an impressionable stock market, it participates more actively in the interplay among stock markets, which results in higher forecasting accuracy for the DCRNN-RV model. Hence, the graphical propagation mechanism of the GNN works better for OMXSPI than for HSI, KS11 and N225, which results in more accurate RV forecasts for OMXSPI. Besides, for the influential stock markets, the DCRNN-RV only fails to achieve significantly more accurate forecast results in SPX once in all the experiments. This is also well explained by the ω value for SPX in Table 15 because, among the influential stock markets, the SPX index has the largest ω value. Since the DCRNN-RV model employs the full volatility spillover effect instead of the net volatility spillover effect, influential stock markets are also influenced by other influential stock markets or even impressionable stock markets. Compared to other influential markets, the SPX exhibits less participation in volatility spillover, resulting in a slightly poorer understanding of its volatility dynamics for the DCRNN-RV model. Furthermore, this finding underscores the importance of bidirectional influences between stock markets. Even for influential markets, incorporating impacts from other markets is crucial for accurate RV forecasting.

| Stock Market Index | ω |
|--------------------|----------|
| SPX | 0.0277 |
| FCHI | 0.00074 |
| FTSE | 0.0152 |
| HSI | 0.03972 |
| OMXSPI | 0.0179 |
| KS11 | 0.04266 |
| GDAXI | 0.00785 |
| N225 | 0.05982 |

Table 15: The ω values for each stock market index

6 Conclusion

This research expands the current state-of-the-art STG-Spillover model by accounting for non-trading days and including the dynamic graph structure in RV forecast for different stock market indices globally. These new designs are also unprecedented in the traditional HAR-RV model and its extensions. In the empirical study, the DCRNN-RV model always generates significantly more accurate forecasts for more than half of the markets involved in the analysis compared to the STG-Spillover model. The design of the changing dynamics of the volatility network and different masks to facilitate graph information propagation is empirically proved to be beneficial for the RV forecast for the chosen stock market indices under all different look-back and forecast window settings. Besides, the idea of using Table 15 to account for the slightly inconsistent forecasting performance can also reflect that the DCRNN-RV model is more sensitive to the underlying interconnection among stock markets so that even the occurrence of unique uncommon trading days plays a role in the RV forecast. This further emphasizes the importance of the comovement or correlation among entities in volatility analysis and the bidirectionality of the volatility spillover effects. In addition, the proposed DCRNN-RV model can generate forecasts on the union of trading days of different stock markets, which ensures it has significant practical utility in actual transactions. The DCRNN-RV model allows stock market participants to consider the influence of all other markets on a given market when investing on uncommon trading days, not just on common trading days.

Hence, it is feasible to conclude that the integration of the uncommon trading days and the dynamic relationship network leads to a more accurate and highly practical RV forecast model and is beneficial for understanding the volatility dynamic for different stock markets.

7 Disclosure of Interest

No conflict of interest is to be declared.

8 Disclosure of Funding

No funding was received.

9 Data Availability Statement

Data were downloaded from Oxford-man Institute's realized library. The authors confirm that the data supporting the findings of this study are available within the supplementary materials of the paper.

References

- Andersen, T. G. and T. Bollerslev (1998). Answering the skeptics: Yes, standard volatility models do provide accurate forecasts. *International Economic Review* 39(4), 885–905.
- Bollerslev, T., B. Hood, J. Huss, and L. H. Pedersen (2018, 05). Risk Everywhere: Modeling and Managing Volatility. *The Review of Financial Studies* 31(7), 2729–2773.
- Bubák, V., E. Kočenda, and F. Žikeš (2011). Volatility transmission in emerging european foreign exchange markets. *Journal of Banking & Finance* 35(11), 2829–2841.
- Cheung, Y.-W. and K. S. Lai (1995). Lag order and critical values of the augmented dickey–fuller test. *Journal of Business & Economic Statistics* 13(3), 277–280.
- Chung, J., C. Gulcehre, K. Cho, and Y. Bengio (2014). Empirical evaluation of gated recurrent neural networks on sequence modeling. *CoRR abs/1412.3555*.
- Corsi, F. (2009, 02). A Simple Approximate Long-Memory Model of Realized Volatility. *Journal of Financial Econometrics* 7(2), 174–196.
- Diebold, F. X. and R. S. Mariano (2002). Comparing predictive accuracy. *Journal of Business & Economic Statistics* 20(1), 134–144.
- Diebold, F. X. and K. Yilmaz (2009, 1). Measuring Financial Asset Return and Volatility Spillovers, with Application to Global Equity Markets. *The Economic Journal* 119(534), 158–171.
- Diebold, F. X. and K. Yilmaz (2012). Better to give than to receive: Predictive directional measurement of volatility spillovers. *International Journal of Forecasting* 28(1), 57–66. Special Section 1: The Predictability of Financial Markets Special Section 2: Credit Risk Modelling and Forecasting.
- Forbes, K. J. and R. Rigobon (2002). No contagion, only interdependence: Measuring stock market comovements. *The Journal of Finance* 57(5), 2223–2261.

- Friedman, J., T. Hastie, and R. Tibshirani (2007, 12). Sparse inverse covariance estimation with the graphical lasso. *Biostatistics* 9(3), 432–441.
- Hansen, P. R. and A. Lunde (2005). A forecast comparison of volatility models: does anything beat a garch(1,1)? *Journal of Applied Econometrics* 20(7), 873–889.
- Hansen, P. R., A. Lunde, and J. M. Nason (2011). The model confidence set. *Econometrica* 79(2), 453–497.
- Harvey, D., S. Leybourne, and P. Newbold (1997). Testing the equality of prediction mean squared errors. *International Journal of Forecasting* 13(2), 281–291.
- Kanas, A. (2000). Volatility spillovers between stock returns and exchange rate changes: International evidence. *Journal of Business Finance & Accounting* 27(3-4), 447–467.
- Li, Y., R. Yu, C. Shahabi, and Y. Liu (2018). Diffusion convolutional recurrent neural network: Data-driven traffic forecasting. In *International Conference on Learning Representations (ICLR '18)*.
- Liang, C., Y. Wei, and Y. Zhang (2020). Is implied volatility more informative for forecasting realized volatility: An international perspective. *Journal of Forecasting* 39(8), 1253–1276.
- MacKinnon, J. G. (1994). Approximate asymptotic distribution functions for unit-root and cointegration tests. *Journal of Business & Economic Statistics* 12(2), 167–176.
- Mitra, S. (2009). A review of volatility and option pricing.
- Poon, S.-H. and C. W. Granger (2003, June). Forecasting volatility in financial markets: A review. *Journal of Economic Literature* 41(2), 478–539.
- Son, B., Y. Lee, S. Park, and J. Lee (2023). Forecasting global stock market volatility: The impact of volatility spillover index in spatial-temporal graph-based model. *Journal of Forecasting* 42(7), 1539–1559.

- Sutskever, I., O. Vinyals, and Q. V. Le (2014). Sequence to sequence learning with neural networks. *Advances in neural information processing systems* 27.
- Wilmott, P. (2013). *Paul Wilmott introduces quantitative finance*. John Wiley & Sons.
- Yang, Z. and Y. Zhou (2017). Quantitative easing and volatility spillovers across countries and asset classes. *Management Science* 63(2), 333–354.
- Zhang, C., X. Pu, M. Cucuringu, and X. Dong (2023). Graph neural networks for forecasting multivariate realized volatility with spillover effects. *arXiv preprint [arXiv:2308.01419](https://arxiv.org/abs/2308.01419)*.